Design of a Robotic Mobility System to Promote Socialization in Children

Xi Chen, Christina Ragonesi, James C. Galloway, Sunil K. Agrawal

***Abstract*— Self-initiated mobility is a causal factor in children's development. Previous studies have demonstrated the effectiveness of our training methods in learning directional driving and navigation. The ultimate goal of mobility training is to enable children to be social, that is, to interact with peers. A powered mobility device was developed that can localize itself, map the environment, plan an obstacle-free path to a goal, and ensure safety of a human driver. Combined with a positioning system, this system is able to apply a force field to train subjects to drive towards an object, a caregiver, a peer, or a group of peers. System feasibility was tested by designing a 'ball chasing' game. Results show that the system is promising in promoting socialization in children.**

I. Introduction

IN typically developing infants, the emergence of independent mobility is associated with advances in perception, cognition, motor, and social skills [1], [4]. Our previous studies have demonstrated success in providing power mobility devices to children with special needs [3], [10], [16], [17] and expediting motor learning of driving skills using a force-feedback joystick [2], [6]. Our results suggest that the use of a force-feedback joystick may yield faster learning than the use of a conventional joystick.

The ultimate goal of our research is to train children with special needs to be social, i.e., to interact with peers and caregivers. Previous studies [16], [17] have shown that although special needs children become more mobile and interactive when driving a powered mobility device, they still may not demonstrate peer-typical socialization. Therefore, we would like to design a robotic mobility system that can promote interaction between peers by combining our mobile robot and haptic technology.

In [6], we have trained children with and without mobility impairments to purposefully and safely navigate indoors while avoiding obstacles using the 'assist-as-needed' force field. However, in this experiment, we only targeted the individual driving skills. No peers were present in the training area. The robot was not able to track any human beings. Moreover, the experiment was done in a fixed maze with fixed goals. The training robot was programmed to navigate only inside this particular maze and does not work if the training course is changed or the goal is moving.

This research is supported by grants from National Science Foundation and National Institute of Health.

Xi Chen, and Christina Ragonesi are PhD students at the University of Delaware, Newark, DE 19716, USA.

James C. Galloway is an Associate Professor in Physical Therapy Department, University of Delaware.

Sunil K. Agrawal is a professor in Mechanical Engineering Department, Columbia University, New York, NY 10027, USA. He is also the corresponding author. Sunil.Agrawal@columbia.edu

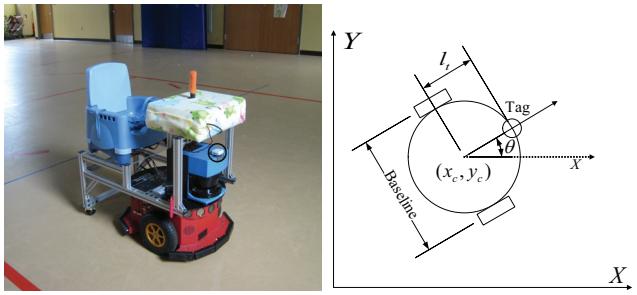

Fig. 1. The robotic mobility device based on Pioneer 3-DX with a Ubisense tracking system that uses tags to locate moving points in space. The figure shows a lidar mounted at the front the robot. The tag is placed on top of the lidar (in the black circle) and $l_t = 0.166$m ahead of the robot.

Several smart wheelchairs are available that are capable of obstacle avoidance, path planning, and shared control [5], [11], [14], [20]. However, all these studies have focused on enhancing individual driving experiences. *To the best knowledge of the authors, this is the first study that attempts to promote socialization in children using a powered mobility device and a tracking system, and demonstrate the feasibility with a ball chasing game.* The system is designed to work in both static and dynamic environments with obstacles and other children. In order to facilitate this game, the robot has to accurately build a map of the environment, know the position of the peers, and then plan paths to follow peers or achieve targeted goal points via a controller. This motion is then mapped to a force-feedback joystick to set up force tunnels to train children to learn this behavior. The robot must also be able to slow down or stop in front of an unexpected obstacle since the motion commands are given by the child using a joystick.

The rest of the paper is organized as follows: Section II describes the experiment setup of the robot hardware and a tracking system. Detailed capabilities of localization, path planning and control, force feedback and safety issues are presented in Sections III, IV, and V respectively. Section VI presents the experiment protocol of a group study with 10 toddlers. Training results and discussions are presented in Section VII followed by conclusion.

II. Experiment Setup

Our robotic mobility device was designed to ensure comfort, performance, and safety (Fig. 1). The base robot is a Pioneer 3-DX, which is equipped with encoders to record the trajectory of the vehicle. A lidar was mounted at the front of the robot to map the environment. The seat was mounted

978-1-4673-6024-1/13/$31.00 ©2013 IEEE

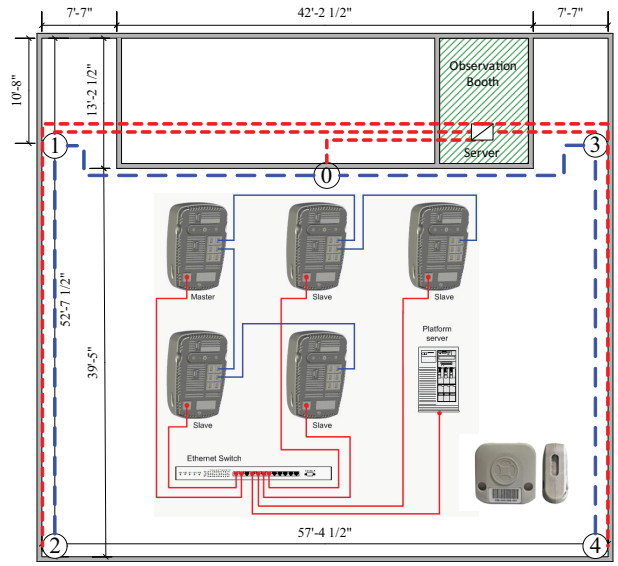

Fig. 2. Floor plan of the gymnasium of the ELC and the Ubisense IPS: receivers and tags. The play area is of rectangular shape. Five receivers are mounted at positions 0-4 and are connected to a computer server by data cables (red) and timing cables (blue).

on an aluminum extruded frame with low inertia, while still providing a stable base for a child to sit on the robot.

There are many approaches available to track humans, using lidar [18], vision [8], or a combination of these [13]. However, these sensors must face the target in order to be effective. This is not always possible since the sensors have a fixed orientation relative to the robot. Since the robot is controlled by a child, it is likely that the robot faces away from the target during motion. Therefore, an Indoor Positioning System (IPS) from Ubisense was used for locating points during the experiment.

The experiments were conducted in the gymnasium of the Early Learning Center (ELC) of the University of Delaware (Fig. 2). Five Ubisense receivers were mounted on the walls around the gymnasium and were connected to a computer server. The target to be tracked carries a tag which emits Ultra Wide Band signals that are picked up by these receivers. The server runs our software using the Ubisense API that can calculate the 3D position of the tag and sends this information, together with the unique tag ID, to the mobile robot through wireless network. In addition, tags can be placed on children moving in the environment. The position of each child and other objects can be identified using the tag ID. The system has the advantage of tracking multiple tags, making it possible to track multiple moving objects and children.

III. Localization

Under the assumption of no-slip in the wheels, the states of a mobile robot satisfy Eq. (1):

$$\begin{cases} \dot{x}_c = v\cos\theta \\ \dot{y}_c = v\sin\theta \\ \dot{\theta} = \omega. \end{cases} \tag{1}$$

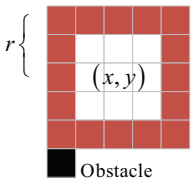

Fig. 3. Clearance of a cell (x, y). The black cell is occupied by an obstacle. The red cells represent the boundary of the obstacle-free square.

where (x_c, y_c) are the coordinates of the robot center and θ is its orientation. However, this no-slip condition is not always satisfied. As the robot moves, the odometer accumulates error. In this study, the IPS readings of the robot are fused with odometry data recorded from the wheel encoders to compensate for slip errors in position of the vehicle.

A Ubisense tag was placed at l_t ahead of the robot. The IPS observes the tag position:

$$\mathbf{y}(t) = \begin{pmatrix} x_c(t) + l_t\cos\theta(t) \\ y_c(t) + l_t\sin\theta(t) \end{pmatrix} \tag{2}$$

Clearly, the tag is mounted at l_t ahead of the robot to make the system fully observable so that all three states of the robot can be updated.

The odometry data was then fused with IPS readings by following the procedure of an Extended Kalman Filter. This algorithm achieved a position accuracy of 0.1m and orientation accuracy of 5 degrees in the experiment. This was calculated by repeated measurements of the estimated robot position at several known fixed locations.

IV. Integrated Path Planning and Control

Since the environment is dynamic, the robot uses a certainty grid map to record static and slow moving obstacles [19]. Several map-based path planning algorithms are available [7] that include potential fields, roadmaps, sampling based algorithms, etc. Planning algorithms on grid maps are typically based on A* or D*. The path planning problem in this study faces the following challenges: i) The environment has slowly moving obstacles, fast moving human subjects, and changing goals. ii) Fast planning is needed, as children become quickly impatient, usually within seconds. iii) The robot follows the joystick command given by the child; it is likely that it will deviate from the desired path. Although many of the algorithms above are capable of dealing with dynamic environments, none of them is designed to cope with the uncertainty due to the driver inputs. A quick recovery technique is needed to avoid unnecessary replanning.

A. Path Planning

In this experiment, inspired by Pathak *et al* [15], an integrated path planning and control approach was developed to plan an obstacle-free path to the moving goal and control the robot autonomously. Unlike [15], the planning algorithm is an online algorithm and does not make assumptions about the shape of the obstacles. In a certainty grid map, it is very convenient to generate an obstacle-free square centered on cell (x, y) instead of a bubble (Fig. 3).

Algorithm 1 getClearSquareSize($Cell$)

Require: cell coordinate (x, y)

Ensure: clearance r of the largest obstacle-free square centered on cell (x, y)

$r = 0$
for all the neighbor n_{nb} with Clearance$(n_{nb}) \neq 0$ **do**
  $r = \min_{\forall n_{nb}} \{\text{Clearance}(n_{nb})\}$
end for
while Square($Cell$,r) is within the map **do**
  if any cell on the 4 sides of Square($Cell$,r) is occupied **then**
    return $r - 1$
  else
    $r = r + 1$
  end if
end while
return $r - 1$

Algorithm 2 Switching strategy

if inside the current square **then**
  if the current square is not the final goal **then**
    if the next goal is not blocked **then**
      Move on to the next goal and return it
    else
      Replan a path
    end if
  else
    Return the current goal
  end if
else
  if the robot is inside the previous square **then**
    Return the current goal
  else
    Replan a path
  end if
end if

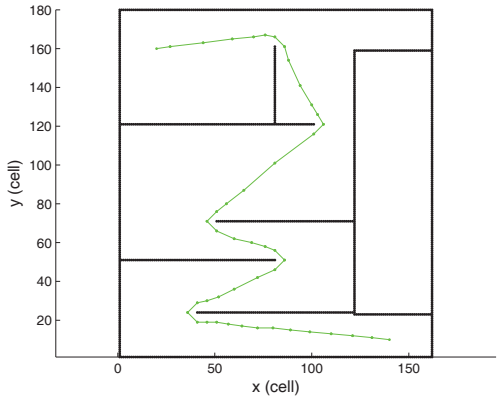

(a) A*+Square Generation

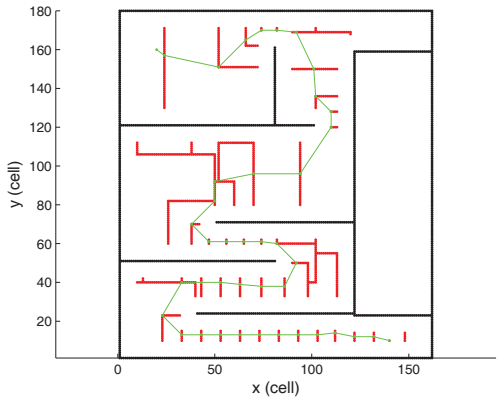

(b) Relaxed A*+Square Generation

Fig. 4. Path planned from cell $(140, 10)$ to $(20, 160)$ in the gymnasium with complex obstacles. (a) Used 18 seconds. (b) Used 0.15 seconds. The red dots represent all the cells that were expanded.

We found that if the square generation is guided by A*, the computation time is too long to be used for training (Fig. 4 (a)), although the resulted path is optimal. Therefore, while still using the heuristic function which is the Euclidean

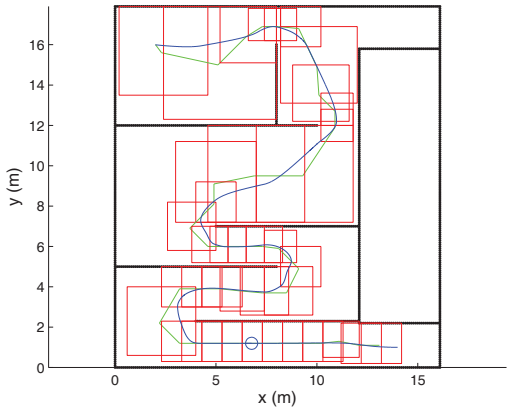

Fig. 5. Simulation of the robot tracking a path planned from $(14\text{m}, 1\text{m})$ to $(2\text{m}, 16\text{m})$. Only static obstacles (in black) are shown. The red lines mark the obstacle-free squares and the green lines are the planned path. The blue line is the actual path traveled.

distance from a cell to the goal, we relax the algorithm by not expanding the cells inside any square which is already on the closed list. Since if a square is generated and placed on the closed list, a good enough path from the start point to this square is already found. By relaxing the algorithm, the computation time is fast and can be used to train children (Fig. 4 (b))

Algorithm 1 generates an obstacle free square centered on cell (x, y), which is an essential step in the path planning algorithm. It starts from the center and checks each of the 4 sides of the square with increasing size. A heuristic method is used here: if a cell has clearance r, the adjacent cell has clearance at least $r - 1$ but at most $r + 1$. This reduces the time complexity of computing the clearance of the adjacent cells from $O(N^2)$ to $O(N)$. If the square size is not large enough for the robot to drive through, this cell will not be expanded, making it convenient to adjust to different sizes of vehicles.

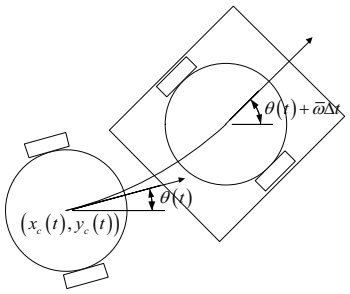

Fig. 6. Pose prediction after executing velocity command (v, ω). A bounding box is also shown around the predicted pose.

Fig. 7. A child driver is driving towards the ball in the ball chasing game.

This path planning algorithm returns a series of intermediate goals from the start to the final goal. The robot simply needs to follow these goals one by one. The eventual path length traveled along this non-optimal plan can be reduced by carefully designing a controller and switching strategy.

B. Controller

Initially, the current square is the square centered on the first intermediate goal, which is the $Start$. Therefore, the robot is always inside the current square initially. The switching strategy is outlined in Algorithm 2. Note that as long as the moving goal is still inside the square, no replanning is needed. As long as the robot is inside some square, the center of the next square is always its next intermediate goal, thus avoiding any ambiguities in path following if the robot deviates from the desired path. Since the center of the next square is always on the edge of the current square, the robot always has a line of sight with the next goal before switching. This eliminates the possibility that the robot will be trapped in local minima.

Once the current goal is determined, the robot can track this goal using the controller in [6]. The attractive potential field is set on the current goal and, if any moving obstacle is inside the current square, the repulsive potential is set according to [6]. Then, the robot globally tracks the goal while locally avoiding obstacles. Figure 5 shows the simulation using this potential field based controller. Note that the zigzag path (in green) is short cut to a much smoother path (in blue) due to the tracking strategy.

V. Human-Robot Interaction and Safety

The desired control input is used to set an 'assist-as-needed' force field on a force-feedback joystick described in [2], [6] to train human subjects. However, since the robot follows commands from the joystick and it is possible that a subject can override the force field, precautions must be taken to prevent the robot from crashing into obstacles.

In this experiment, the maximum velocity of the robot can be as high as 0.5m/s. Due to the dynamic constraint, the robot cannot immediately reach any set velocity. Therefore, system dynamics must be considered. Inspired by the dynamic window approach [9], the robot pose after executing a velocity command (v, ω) is predicted and checked for collision (Fig. 6). The maximum translational acceleration is $a_v = 0.3\mathrm{m/s}^2$ and the maximum rotational acceleration is $a_\omega = 100\mathrm{deg/s}^2$ for Pioneer3-DX robot. A velocity command (v, ω) is considered to be safe if, after executing (v, ω) for 1 control cycle and $(0, 0)$ for all the following cycles, the robot does not collide into obstacles. Therefore, the robot pose is estimated in 2 steps.

1) Predict the robot velocity in 1 cycle after executing (v, ω) given the velocity (v_0, ω_0) at time t:

$$v_1 = \begin{cases} v_0 + a_v \Delta t & \text{if } \frac{v - v_0}{a_v \Delta t} > 1 \\ v & \text{otherwise} \end{cases}$$
$$\omega_1 = \begin{cases} \omega_0 + a_\omega \Delta t & \text{if } \frac{\omega - \omega_0}{a_\omega \Delta t} > 1 \\ \omega & \text{otherwise} \end{cases} \quad (3)$$

where $\Delta t = 0.1$s is the control cycle for Pioneer3-DX robot. Then, the robot pose in 1 cycle after executing (v, ω) is predicted by:

$$\begin{cases} x_c(t + \Delta t) = x_c(t) + \frac{v_0 + v_1}{2} \Delta t \cos \frac{\theta(t) + \theta(t + \Delta t)}{2} \\ y_c(t + \Delta t) = y_c(t) + \frac{v_0 + v_1}{2} \Delta t \sin \frac{\theta(t) + \theta(t + \Delta t)}{2} \\ \theta(t + \Delta t) = \theta(t) + \frac{\omega_0 + \omega_1}{2} \Delta t \end{cases} \quad (4)$$

2) Predict the robot pose after a full stop by executing $(v = 0, \omega = 0)$, using the equations above with:

$$\Delta t = \max \left\{ \frac{v_1}{a_v}, \frac{\omega_1}{a_\omega} \right\} \quad (5)$$

Then if none of the cells inside the bounding box (Fig. 6) is occupied, the current velocity command is considered safe and is sent to the motor controller. Otherwise, a stop command $(0, 0)$ is given.

VI. Experiment Protocol

A ball chasing game was designed to test the system feasibility. In this game, a caregiver and some children pass a ball to each other at one side of the gymnasium and attract a child driver to the ball (Fig. 7). If the driver successfully reaches the group, the ball will be passed to him/her. The driver and the ball were separated by at least 5m at the beginning of each trial. A Ubisense tag was installed inside the ball so that the robot always knows the ball position and can plan an obstacle-free path to the ball.

The experiment was conducted on 10 typically-developing children, 2-3 years old, assigned randomly into two groups.

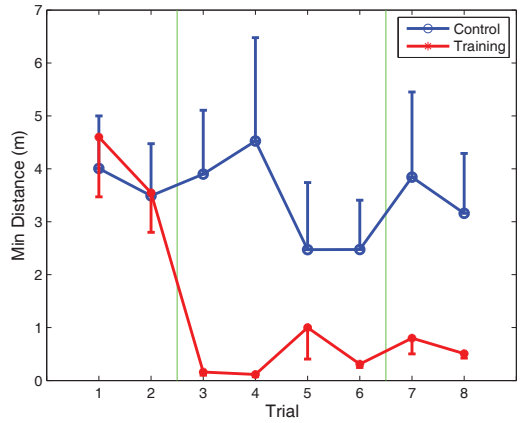

Fig. 8. Mininum distance of the two groups over 8 trials. Error bar shows 1 Standard Error. Trial 1-2 are the baseline. Trial 3-6 are the training trials. Trial 7-8 are the post-training trials.

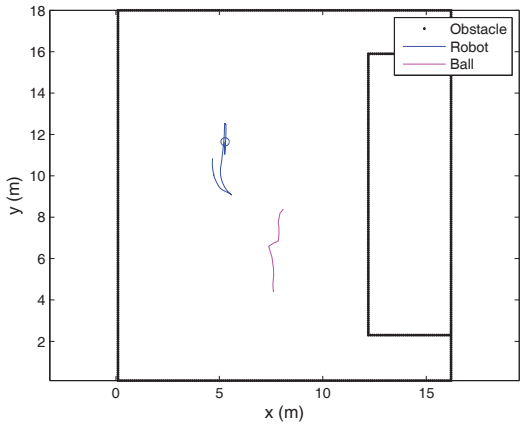

Fig. 9. A typical training trial of the control group. The child driver started at $(5.28, 11.64)$ and was supposed to get the ball at $(7.50, 6.00)$. The ball moved around with the caregiver and some peers to attract the driver.

The training group included 5 toddlers with an average age of 2.56 ± 0.26 years and were trained to drive with the force field. The control group also included 5 toddlers with an average age of 2.66 ± 0.28 years, who drove without the force field. The parents of all children signed a consent form approved by the Institutional Review Board of the University of Delaware. The experiment consisted of three sets of movements on a single day.

1) Baseline: 2 trials without the force field were collected for both groups.
2) Training: Children in the training group were trained with the force field for 4 trials while children in the control group operated without the force field for 4 trials.
3) Post-training: 2 trials without the force field were collected for both groups.

Each trial ended in a minute, or if the child successfully got the ball, whichever occurred first. During each trial, the robot pose and the ball position were recorded for data

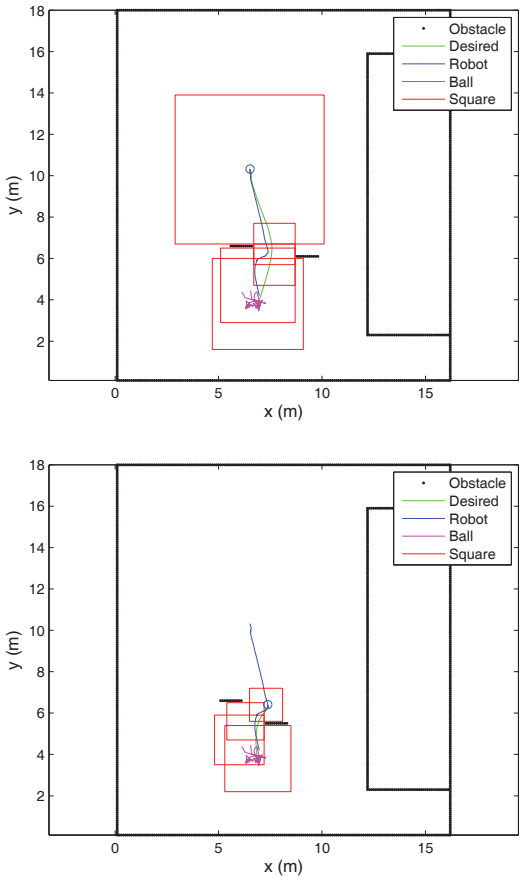

Fig. 10. A typical training trial of the training group. The child driver started at $(6.52, 10.32)$ and was supposed to get the ball at $(6.90, 3.80)$. (Up) A desired path was planned at the beginning of the trial to pass two moving obstacles towards the ball. (Down) As the robot moved forward, the right obstacle moved in the way. An new desired path was planned to the ball.

analysis. The minimum distance from the robot to the ball during each trial was calculated as the outcome measure to compare the performance of the two groups.

VII. Results and Discussion

Figure 8 shows the minimum distance over 8 trials for both groups. During the baseline, the performances of the two groups were almost the same. With the force field turned on, the minimum distance of the training group to the ball was significantly lower than the baseline (paired t-test on the minimum distance during Trial 3 and Trial 2, $p = 0.011$). This did not happen with the control group.

Figure 9 shows a typical training trial from the control group. The driver failed to join the group to play with the ball within 1 minute. Figure 10 shows a typical training trial from the training group. The figure on the top shows that at the beginning of the trial, a series of obstacle-free squares was generated to the ball and pass the two moving obstacles (peers in the gymnasium). If the robot moved autonomously, the resulted path would have been the same as the desired path (in green). Since the robot was driven by a child driver,

the actual path deviated from the desired path. However, as long as the robot is within any square, no replanning will be needed. The figure at the bottom shows that as the robot moved forward, the right peer moved in the way of the desired path. The robot detected this event and according to Algorithm 2, a new series of obstacle-free square was generated. Eventually, the child succeeded in joining the group and playing the ball. These indicate that all the system modules functioned well and the force field helped the child to drive closer to the ball. Note that although the goal was constantly moving, no replanning was needed since the goal was always inside its square.

Toddlers in the training group also showed short-term learning due to the force field. After the training, the minimum distance was significantly lower than the baseline (paired t-test on the minimum distance during Trial 8 and Trial 2, $p = 0.019$) for the training group. There was no significant difference between the baseline and post-training trials for the control group ($p = 0.804$). In fact, all of the children in the training group got the ball in most of the training and post-training trials. Only some of the children in the control group got the ball and this was only for a couple of trials out of 8.

VIII. Conclusion

This is the first study that attempts to promote socialization in children by designing a robotic mobility device with a tracking system. The powered mobility device is able to accurately localize itself in the training environment, map obstacles, plan a path to a goal, set a force field according to the executed path to train subjects to drive towards the goal, and prevent the driver from running into obstacles. The tracking system is capable of tracking multiple targets. By combing our 'assist-as-needed' haptic algorithm, the system can be used to train children to interact with caregivers and peers. A ball chasing game was developed as a simple, standardizable activity that would model a likely social scenario for children. System functions and feasibility were tested by a group study involving 10 toddlers. Results showed that all system modules functioned well. Children in the training group drove closer to the ball possessed by a group of peers with the help of the force field and also demonstrated short-term learning.

In this experiment, the goal was to go to the ball. However, in real life, the same tracking system can be creatively implemented to encourage or train a child to drive to his/her peers, teachers, etc. It is possible that keeping close to and playing with peers is more important than simply learning to drive towards peers. Interaction with peers is the most desirable outcome measure, as well as developmental scores and psychological assessment. These will be explored in the future using this system.

ACKNOWLEDGMENTS

We would like to thank Steve Beard for his assistance in fabricating the device at the machine shop. We acknowledge financial support from the National Institute of Health under Grant No. HD047468 and from the National Science Foundation under Grant No. NSF0745833.

References

[1] Anderson, D.I., Campos, J.J., Anderson, D.E., Thomas, T.D., Witherington, D.C., Uchiyama, I., Barbru-Roth, M.A., *The Flip Side of Perception-action Coupling: Locomotor Experience and the Ontogeny of Visual-postural Coupling*, Hum Mov Sci, 20(4-5):461-487, 2001.

[2] Agrawal, S.K., Chen, X., Ragonesi, C., Galloway, J.C., *Training Toddlers Seated on Mobile Robots to Steer Using Force-Feedback Joystick*, IEEE Trans. Haptics, *In Press*, 2011.

[3] Agrawal, S.K., Chen, X., Kim, M.J., Lee, Y.M., Cho, H.P., Park, G.J., *Feasibility Study of Robot Enhanced Mobility in Children with Cerebral Palsy*, Proc. IEEE Int. Conf. Biomedical Robotics and Biomechatronics, 2012.

[4] Campos, J.J., Anderson, D.I., Barbu-Roth, M.A., Hubbard, E.M., Hertenstein, M.J., Witherington, D., *Travel Broadens the Mind*, Infancy, 1(2):149-219, 2000.

[5] Carlson, T., Demiris, Y., *Collaborative Control for a Robotic Wheelchair: Evaluation of Performance, Attention, and Workload*, IEEE Trans Syst Man Cybern B, 42(3):876-88, 2012.

[6] Chen, X., Ragonesi, C., Agrawal, S.K., Galloway, J.C., *Training Toddlers Seated on Mobile Robots to Drive Indoors Amidst Obstacles*, IEEE Trans. Neural Systems and Rehabilitation Engineering, 19(3):271-279, 2011.

[7] Choset, H., Lynch, K.M., Hutchinson, S., Kantor, G., Burgard, W., Kavraki, L.E., Thrun, S., *Principles of Robot Motion: Theory, Algorithms, and Implementations*, The MIT Press, Boston, 2005.

[8] Dalal, N., Triggs, B., *Histograms of Oriented Gradients for Human Detection*, Proc. IEEE Computer Society Conf. Computer Vision and Pattern Recognition, 1, 886-893, 2005.

[9] Fox, D., Burgard, W., Thrun, S., *The Dynamic Window Approach to Collision Avoidance*, IEEE Robot Autom Mag, 4(1):23-33, 1997.

[10] Galloway, J.C., Ryu, J.C., Agrawal, S.K., *Babies Driving Robots: Self-generated Mobility in very Young Infants*, Intel Serv Robotics, 1(2):123C134, 2008.

[11] Katevas, N.I., Sgouros, N.M., Tzafestas, S.G., Papakonstantinou, G., Beattie, P., Bishop, J.M., Tsanakas, P., Koutsouris, D., *The Autonomous Mobile Robot SENARIO: a Sensor Aided Intelligent Navigation System for Powered Wheelchairs*, IEEE Robot Autom Mag, 4(4):60-70, 1997.

[12] Kleeman, L., *Advanced Sonar and Odometry Error Modeling for Simultaneous Localisation and Map Building*, Proc. IEEE/RSJ Int. Conf. Intelligent Robots and Systems, 1, 699-704, 2003.

[13] Kobilarov, M., Sukhatme, G., Hyams, J., Batavia, P., *People Tracking and Following with Mobile Robot Using an Omnidirectional Camera and a Laser*, Proc. IEEE Int. Conf. Robotics and Automation, 557-562, 2006,

[14] Montesano, L., Diaz, M., Bhaskar, S., Minguez, J., *Towards an Intelligent Wheelchair System for Users With Cerebral Palsy*, IEEE Trans. Neural Systems and Rehabilitation Engineering, 18(2):193-202, 2010.

[15] Pathak, K., Agrawal, S.K., *An Integrated Path-planning and Control Approach for Nonholonomic Unicycles Using Switched Local Potentials*, IEEE Trans. Robotics, 21(6):1201-1208, 2005.

[16] Ragonesi, C., Chen, X., Agrawal, S.K., Galloway, J.C., *Power Mobility and Socialization in Preschool: A Case Report on a Child with Cerebral Palsy*, Pediatric Physical Therapy, 22(3):322-329, 2010.

[17] Ragonesi, C.B., Chen, X., Agrawal, S.K., Galloway, J.C., *Power Mobility and Socialization in Preschool: Follow-up Case Study of a Child With Cerebral Palsy*, Pediatr Phys Ther, 23(4):399-406, 2011.

[18] Schulz, D., Burgard, W., Fox, D., Cremers, A.B., *Tracking Multiple Moving Targets with a Mobile Robot Using Particle Filters and Statistical Data Association*, Proc. IEEE Int. Conf. Robotics and Automation, 2, 1665-1670, 2001.

[19] Thrun, S., *Learning Metric-topological Maps for Indoor Mobile Robot Navigation*, Artificial Intelligence, 99(1):21-71, 1998.

[20] Zeng, Q., Teo, C.L., Rebsamen, B., Burdet, E., *A Collaborative Wheelchair System*, IEEE Trans. Neural Sysyems and Rehabilitation Engineering, 16(2):161-170, 2008.